Heliyon 10 (2024) e39871

Contents lists available at ScienceDirect

Heliyon

journal homepage: www.cell.com/heliyon

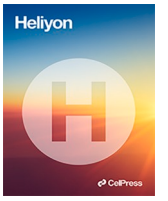

Research article

High-fat and high-carbohydrate diets worsen the mouse brain susceptibility to damage produced by enterohemorrhagic *Escherichia coli* Shiga toxin 2

D. Arenas-Mosquera [a], N. Cerny [b,c], A. Cangelosi [d], P.A. Geoghegan [d], E.L. Malchiodi [e], M. De Marzi [f], A. Pinto [a,**,1], J. Goldstein [a,*,1]

[a] *Universidad de Buenos Aires, Consejo Nacional de Investigaciones Científicas y Técnicas (CONICET), Instituto de Fisiología y Biofísica ''Houssay" (IFIBIO), Laboratorio de Neurofisiopatología, Facultad de Medicina, Paraguay 2155 Piso 7, 1121, Ciudad de Buenos Aires, Argentina*
[b] *Universidad de Buenos Aires, Facultad de Farmacia y Bioquímica, Cátedra de Inmunología e Instituto de Estudios de La Inmunidad Humoral (IDEHU), UBA-CONICET, Junín 956 Piso 4, 1113, Ciudad de Buenos Aires, Argentina*
[c] *Universidad de Buenos Aires, Facultad de Medicina, Departamento de Microbiología, Parasitología e Inmunología e Instituto de Microbiología y Parasitología Médica (IMPaM), UBA-CONICET, Paraguay 2155 Piso 12, 1121, Ciudad de Buenos Aires, Argentina*
[d] *Centro Nacional de Control de Calidad de Biológicos (CNCCB), "ANLIS, Dr. Carlos G. Malbrán", Avenida Vélez Sarsfield 563, 1282, Ciudad de Buenos Aires, Argentina*
[e] *Universidad de Buenos Aires, IDEHU-CONICET, Facultad de Farmacia y Bioquímica, Cátedra de Inmunología, Junín 956, Piso 4°, 1113, Ciudad de Buenos Aires, Argentina*
[f] *Universidad Nacional de Luján, Departamento de Ciencias Básicas, Ruta 5 y Avenida Constitución (6700) Luján, Buenos Aires, Argentina, Universidad Nacional de Luján, Instituto de Ecología y Desarrollo Sustentable (INEDES)-CONICET, Laboratorio de Inmunología, Ruta 5 y Avenida Constitución (6700) Luján, Buenos Aires, Argentina*

A R T I C L E I N F O

Keywords:
High fat diet
High carbohydrate diet
Brain
Thalamus
Shiga toxin
Hemolytic uremic syndrome
Inflammation
Neurodegeneration
Astrocyte reactivity
Microglial reactivity

A B S T R A C T

Background: Nutrition quality could be one of the reasons why, in the face of a Shiga toxin-producing enterohemorrhagic *Escherichia coli* outbreak, some patients experience more profound deleterious effects than others, including unfortunate deaths. Thus, the aim of this study was to determine whether high-fat and/or high-carbohydrate diets could negatively modulate the deleterious action of Shiga toxin 2 on ventral anterior and ventral lateral thalamic nuclei and the internal capsule, the neurological centers responsible for motor activity.
Methods: Mice were fed a regular, high-fat, high-carbohydrate diet or a combination of both previous to the intravenous administration of Shiga toxin 2 or vehicle. Four days after intravenous administration, mice were subjected to behavioral tests and then sacrificed for histological and immunofluorescence assays to determine alterations in the neurovascular unit at the cellular and functional levels. Statistical analysis was performed using one-way analysis of variance followed by Bonferroni *post hoc* test. The criterion for significance was $p = 0.0001$ for all experiments.
Results: The high-fat and the high-carbohydrate diets significantly heightened the deleterious effect of Stx2, while the combination of both diets yielded the worst results, including endothelial glycocalyx and oligodendrocyte alterations, astrocyte and microglial reactivity, neurodegeneration, and motor and sensitivity impairment.

* Corresponding author. Instituto de Fisiología y Biofísica "Houssay", IFIBIO Facultad de Medicina Universidad de Buenos Aires/Conicet Paraguay 2155 piso 7 sector M3 Ciudad de Buenos Aires, Argentina.
** Corresponding author.
E-mail addresses: apinto@fmed.uba.ar (A. Pinto), jogol@fmed.uba.ar (J. Goldstein).
[1] These authors contributed equally.

https://doi.org/10.1016/j.heliyon.2024.e39871
Received 20 May 2024; Received in revised form 21 October 2024; Accepted 25 October 2024
Available online 26 October 2024
2405-8440/© 2024 Published by Elsevier Ltd. This is an open access article under the CC BY-NC-ND license (http://creativecommons.org/licenses/by-nc-nd/4.0/).

Conclusions: In view of the results presented here, poor nutrition could negatively influence patients affected by Stx2 at a neurological level. Systemic effects, however, cannot be ruled out.

1. Introduction

Shiga toxin (Stx) from Stx-producing *Escherichia coli* (STEC) is the virulence factor responsible for hemorrhagic colitis, hemolytic uremic syndrome (HUS), and associated acute encephalopathy, triggered by the presence of STEC in food, water, or cross-contamination. When the central nervous system (CNS) is compromised, mortality rates increase significantly [1].

Stx2 is encoded by a lambda bacteriophage. Through the activation of the SOS response in bacteria, the *Stx2* gene undergoes excision and replication, and Stx2 is then expressed and released [2–4]. It is well accepted that Stx2 produces its deleterious effect via its canonical cell membrane receptor globotriaosylceramide (Gb3) [5]. Our group and others have reported the localization of this receptor in neurons and microglia in the CNS [1,5,6]. In addition, Gb3 is upregulated following Stx2 administration, concomitantly with a wide range of neurological alterations [5,7–9]. Acute encephalopathy is a sign of poor prognosis which increases mortality rates in children suffering from HUS [10]. Neurological injury reports include decerebrate posture, hemiparesis, ataxia and cranial nerve palsy, hallucinations, seizures, and changes in the level of consciousness (from lethargy to coma) [11,12]. Similar signs of neurological impairment like lethargy, shivering, abnormal gait, hindlimb paralysis, spasm-like seizures, reduced spontaneous motor activity, and pelvic elevation have been observed in mouse models of HUS encephalopathy [6,13].

Among the CNS areas affected in patients with HUS encephalopathy, the thalamus presents the most severe damage [8,14–16]. Patients usually exhibit symmetrical hyper-intensities of thalamic magnetic resonance imaging, which is consistent with thalamic damage [14–16]. Neurological signs comprise alterations in consciousness, cognitive dysfunction –attention, orientation, working or short-term memory deficits–, and apraxia. Additional clinical signs include headaches and focal neurological deficits such as extra pyramidal, cerebellar, or brainstem symptoms [8]. All these clinical manifestations may reflect thalamic impairment, since it is a relay structure that connects the major ascending and descending neurologic pathways.

Strikingly, it is not clear why only 20 % of children infected with STEC develop HUS, with 5 % of these children also developing HUS-associated encephalopathy [1]. A plausible explanation may lie in poor nutrition based on a high-fat and/or high-carbohydrate diet, consistent with a chronic systemic pro-inflammatory state and increased oxidative stress [17]. We therefore hypothesize that the quality of a high-fat and/or high-carbohydrate diet in children suffering STEC may determine the severity of HUS encephalopathy. For these reasons, the object of this study is to determine whether high-fat and/or high-carbohydrate diets worsen the deleterious effects of Stx2 on thalamic ventral anterior and ventral lateral nuclei (VAVL), and the internal capsule [18] on neurovascular units responsible for motor activity in mice, particularly an ascending pathway connecting fibers from the thalamus to the cerebral cortex [19]. This work also aims to determine a possible proinflammatory involvement in the effects of Stx2 and whether the changes observed at a cellular level are associated with mouse behavior. This work may thus help elucidate the series of events taking place in a translational murine model of STEC contamination that mimics clinical events from a dietary perspective.

2. Methods

2.1. Animals

Male NIH Swiss mice were housed under 12h-light/12h-dark conditions. Food and water were provided *ad libitum* (as described below), and the experimental protocols and euthanasia procedures were reviewed and approved by the Institutional Committee for the Care and Use of Laboratory Animals of the School of Medicine, Universidad de Buenos Aires, Argentina (Resolution N° 3020/2019). All the procedures were performed in accordance with the ARRIVE and EEC guidelines for the care and use of experimental animals (EEC Council 86/609).

2.2. Diets

Twenty one-day-old weaning mice were divided into four groups according to their diet composition (Asociación de Cooperativas Argentinas, San Nicolás, Buenos Aires, Argentina) as follows (Table 1): control normal diet (ND); high-fat diet (HF) consisting of a ND enriched with an additional 37.97 % fat; high-carbohydrate (HC) consisting of a ND enriched with 10 % saccharose solution (#9789.08, Biopack, Buenos Aires, Argentina); and a combined HF + HC diet. After the weaning day, the four diets were administered

Table 1
Nutritional composition for the four groups (%).

Source	ND	HF	HC	HF + HC
Protein	32.57	17.93	32.57	17.93
Carbohydrate	60.49	37.59	60.49	37.59
Fat	6.50	44.47	6.50	44.47
Saccharose	_____	_____	10.00	10.00

for 25 days until the end of the protocol. On day 21 (experimental day zero), animals were subjected to intravenous (i.v.) administration (100 μl) of either Stx2 (1 ng) or vehicle (saline solution). The Stx2 dose was about 60 % of the LD_{50} (1.6 ng per mice). Thus, each diet group (ND, HF, HC and HF + HC) was in turn divided into two i.v. treatments (+veh or + Stx2, n = 10). Four days after i.v. treatment, animals were subjected to behavioral tests and then sacrificed for immunofluorescence assays.

2.3. Swimming test

A swimming test apparatus was built to evaluate mouse motor behavior. The apparatus consisted of a glass tank of 100-cm length, 6-cm width, and 30-cm depth, filled with water (23 °C) up to 10 cm from the top. A visible escape platform was placed 0.5 cm above water at the end of the apparatus. On the opposite side of the escape platform, a vertical dotted black line was drawn 60 cm from the platform. This line served as the start line for recording swimming performance. For this purpose, each mouse was placed before the vertical dotted black line and learned to swim straight into the visible escape platform on the opposite side after two trials. Mouse performance was recorded, and the latency to swim the 60-cm distance was registered.

The swimming test is a valuable tool to assess mouse motor performance by measuring latency of platform escape. This test helps to detect abnormal posture or altered kicking movements in treated animals as compared to coordinated, synchronized paddling movements in control ones. The swimming test is then useful in detecting motor alterations which other tests –like rotarod or gait– fail to detect [20]. Consequently, malnourished mice treated with Stx2 in our study swam more slowly than controls. Regarding limitations, however, motor alterations here correlated with thalamic damage, but other motor regions may also be damaged which the swimming test cannot discriminate.

2.4. Von Frey test

To determine mouse sensitivity, paw withdrawal to mechanical stimuli was measured using the Von Frey test. The test consisted of a 0.7-cm x 0.7-cm chamber in which mice were placed on top of a wire rack with a 10-cm x 12.5-cm grid and allowed to move freely. Animals were habituated to the chamber for 5 min before mechanical stimuli were applied.

The hind paw withdrawal threshold was determined using a sequence of ascending mechanical stimuli (expressed in grams) of calibrated von Frey monofilaments. Twenty filaments ranging from 1.65 g to 6.65 g were used by experimenters who were blinded to mouse treatment allocation. Stimuli were applied in the central region of the plantar surface, avoiding the foot pads. The filament was applied only when the mouse was stationary and standing on all four paws. The withdrawal response was considered valid only if the hind paw was completely removed from the platform. The threshold was determined on the right hind limb.

The von Frey test –in which filaments graded according to their mechanical strength are used to poke the animal's hind paws– remains the gold standard for determining mechanical sensitivity thresholds in murine models. The test presents some limitations, however, in measuring the latency of the response or ensuring reproducibility [21]. Also, the von Frey test cannot accurately determine the type of motor neurons affected.

2.5. Treatments and sample processing

After swimming and Von Frey tests, animals were sacrificed, and brains were processed for histological and immunofluorescence assays. Briefly, mice were anesthetized with pentobarbital (100 mg/kg) and intracardially perfused with paraformaldehyde 4 % in phosphate buffer saline (PBS) 0.1M (pH 7.4) at 4 °C. Brains were removed from the skull, post-fixed with the same solution overnight, and cryopreserved with sucrose solutions at three different concentrations (10, 20 and 30 %) overnight. Coronal sections of 20 μm were obtained on a cryostat and stored in a cryopreserved solution (30 % ethylene glycol and 20 % glycerol in PBS 0.1M) at −20 °C until the day of the assays.

2.6. Histological and immunofluorescence assays

To determine the effect of Stx2 on vascular endothelial cells, brain slices were incubated with biotinylated lectin (10 μg/ml in PBS 0.1M with 0.3 % Triton X-100; Sigma, St. Louis, MO, USA) for 24 h at 4 °C and subsequently incubated with streptavidin Alexa-488 (Invitrogen Molecular Probes, Carlsbad, CA, USA) in a 1:500 dilution for 1 h at room temperature.

To determine the effect of Stx2 on neurons, astrocytes, microglia and oligodendrocytes, brain slices were incubated with mouse neuronal nuclei antibody (anti-NeuN, 1:500; Millipore, Temecula, CA, USA), rabbit glial fibrillary acidic protein antibody (anti-GFAP,1:500; Dako, Glostrup, Denmark), goat ionized calcium binding adaptor molecule 1 antibody (anti-Iba1,1:500; Millipore), and mouse myelin basic protein antibody (anti-MBP, 1:500, Dako, Glostrup, Denmark), respectively for 24 h at 4 °C. After several washes, slices were incubated with their respective secondary antibodies: goat anti-mouse Alexa Fluor 555 (1:500; Amersham, GE, Piscataway, NJ, USA), goat IgG anti-rabbit Alexa Fluor 555 (Invitrogen Molecular Probes, Carlsbad, CA, USA), and donkey anti-goat Alexa Fluor 488 (1:500; Millipore). Hoechst 33342 (1:500; Sigma) was used in all histological and immunofluorescence assays to detect cell nuclei.

The areas chosen in histological and immunofluorescence sections were observed with an Olympus BX50 epifluorescence microscope provided with a Cool-Snap digital camera and a confocal Olympus FV1000 microscope.

Immunostaining is a widely used technique for localizing and quantifying proteins within cells and tissues. Fluorescent markers are sensitive, have a variety of colors, and high resolution. Despite its advantages, the method presents technical challenges such as fixation, permeabilization, and antibody incubation times. The indirect method is time-consuming, generates background noise, and

can cause aberrant crosslinking. Also, fluorescent markers may suffer from background noise, low photostability, quenching, and photobleaching, which makes antibody specificity tests and adequate controls essential [22].

2.7. Image analysis

All micrographs were analyzed using NIH FIJI ImageJ software. For lectin, a scale was first set up using a Neubauer chamber. Next, 8-bit newly transformed micrographs were adjusted with the "threshold" tool and then analyzed with the "set measurements" tool. The number and percentage of lectin-positive particles were then determined. The "cell counter" plugin was used to establish the percentage of morphologically damaged nuclei-neurons and the number of Iba1-positive cells. The "ROI manager" tool was used to establish the expression levels of GFAP, MBP, and Iba1.

2.8. Statistical analysis

The data are presented as the mean ± SEM. In all assays, statistical analyses were conducted using one-way analysis of variance

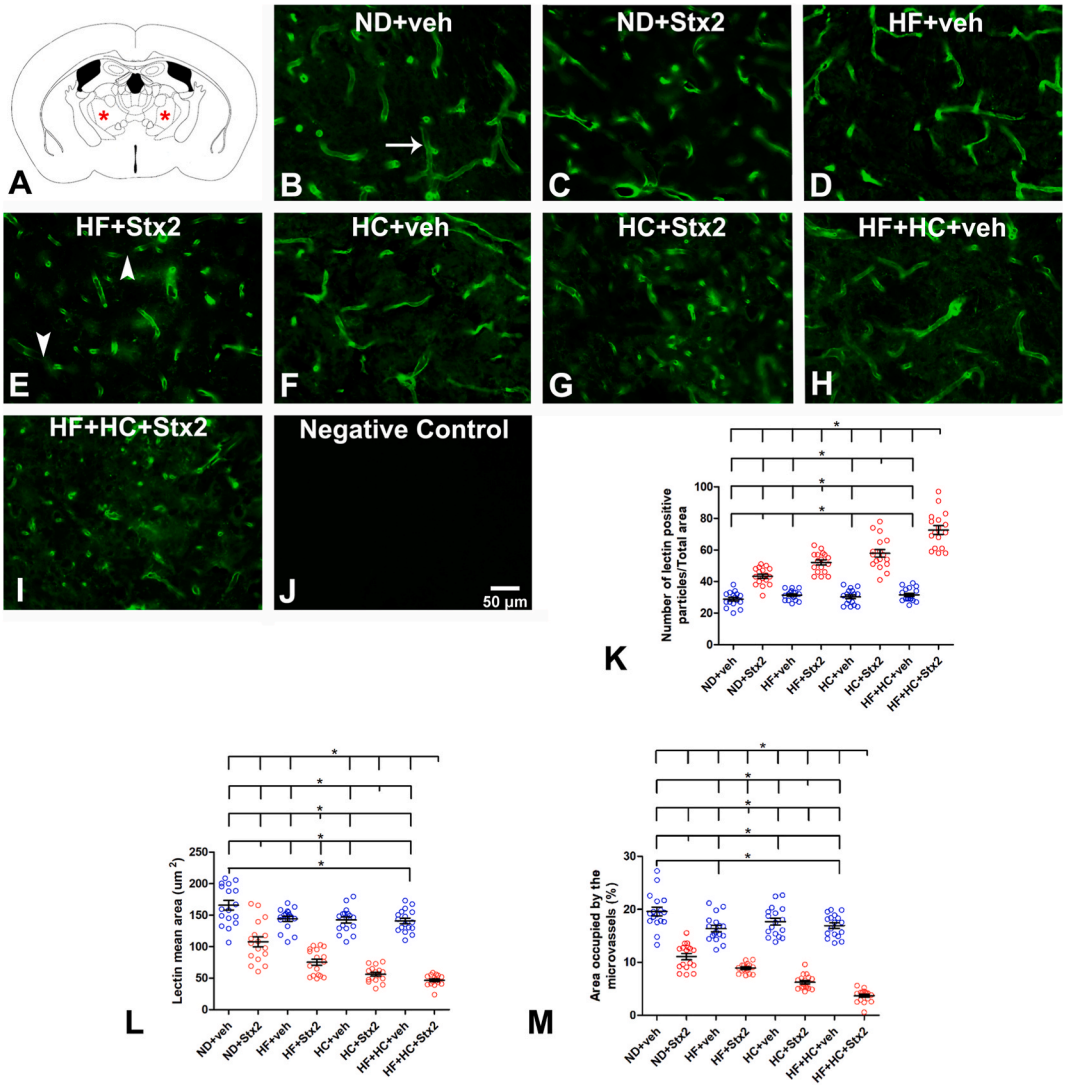

Fig. 1. Changes in microvasculature lectin fluorescence pattern. A: the murine VA-VL brain area studied; B: micrograph shows the microvasculature profile in the ND + veh control group; C: ND + Stx2 treatment; D: HF + veh treatment; E: HF + Stx2 treatment; F: HC + veh treatment; G: HC + Sxt2 treatment; H: HF + HC + veh; I: HF + HC + Stx2; J: negative control by not adding Lycopersicum esculentum lectins; K: number of lectin-immunopositive particles; L: size of microvessels (μm2); M: area occupied by microvessels (%); arrow in B: a conserve microvessel; arrowheads in E: fragmented microvessels. Data were analyzed by one-way ANOVA and Bonferroni post hoc test, $p = 0.0001$, $n = 5$. Scale bar in J applies to all panels.

(ANOVA) followed by Bonferroni *post hoc* test (GraphPad Prism 8, GraphPad Software, Inc., San Diego, CA, USA) between i.v. treatments (control and Stx2). The criterion for significance was $p < 0.0001$ for all experiments.

3. Results

3.1. The HF and/or HC diets heightened Stx2-induced alterations in the microvessel profile

The VA and VL thalamus are analyzed in the present work (Fig. 1A). Lectin from *Lycopersicum esculentum* was used to observe the morphological pattern changes of microvessels produced by Stx2 in each diet, as this compound binds to the glycocalyx present in the luminal membrane of endothelial cells. Parameters evaluated through lectin histofluorescence included the number of lectin-positive particles (Fig. 1K), microvessel size (Fig. 1L), and percentage of area occupied by microvessels (Fig. 1M).

3.1.1. Microvessel assessment in diet groups treated with vehicle

The ND + veh thalamus displayed a conserved profile with a regular lectin fluorescence mark throughout microvessels (Fig. 1B, arrow). The number of microvessels bound to lectins- (Table 2) observed as histofluorescent lectin-positive particles− showed no significant differences across veh-treated diet groups (Fig. 1K), as seen in panels of Fig. 1B–D, F, H.

However, microvessel size (Table 3) was significantly smaller in HF + HC + veh (Fig. 1H) than in ND + veh mice (Fig. 1B), with no significant differences between ND + veh (Fig. 1B), HF + veh (Fig. 1D), or HC + veh (Fig. 1H) mice, Fig. 1L.

Finally, the percentage of area occupied by microvessels was significantly smaller in HF + veh (Fig. 1D) and HF + HC + veh (Fig. 1H), as compared to ND + veh mice (Fig. 1B) (Table 4, Fig. 1M). Surprisingly, HF and HF + HC diets reduced the area occupied by microvessels regardless of Stx2 administration.

3.1.2. Microvessel assessment in diet groups treated with Stx2

We have previously reported that the administration of a sublethal dose of Stx2 alters the microvessel profile [8]. In the present study, Stx2 administration combined with HF and/or HC diets further worsened the microvessel profile, as observed in HF + veh, HC + veh and HF + HC + veh mice (Fig. 1B–I). Indeed, Stx2 administration combined with the HF + HC diet induced a peak in the number of histofluorescent lectin-positive particles (fragmented particles) (Fig. 1K), followed by HF + Stx2 and HC + Stx2 as compared to their respective controls (Table 2, Fig. 1K).

Stx2-treated mice showed microvessels with non-continuous fluorescence labeling (Fig. 1E arrowheads). As a distinct feature of microvessel injury, these non-continuous fluorescence microvessels have been proven smaller in Stx2-treated thalami than in controls [8]. In our work, microvessel size reached the lowest value in HF + HC + Stx2 mice, followed by HF + Stx2 and HC + Stx2 (Table 3, Fig. 1L).

Furthermore, the total area occupied by microvessels was significantly smaller in Stx2-treated mice, as observed in other brain areas [8,9]. The HF + HC + Stx2 group rendered the smallest area, followed by HF + Stx2 and HC + Stx2 (Table 4, Fig. 1M). On the other hand, no lectin histofluorescence binding was found in negative controls (Fig. 1J).

3.2. The HF + HC diet magnified Stx2-induced astrocyte reactivity

To determine the effect of HF and/or HC diets on astrocyte reactivity, GFAP expression was assessed in these cells in the internal capsule (Fig. 2A); this region consists of afferent and efferent cortical fibers, the anterior part containing ascending thalamic projections [23]. Significant astrocyte reactivity was observed in the four diet groups after Stx2 treatment as compared to their respective veh-treated groups (Table 5, Fig. 2B–K). Maximal astrocyte reactivity was found in the HF + HC + Stx2 group, with no significant differences across the other Stx2-treated groups (Fig. 2C–E, G, I). Finally, no GFAP immunofluorescence was observed in negative controls (Fig. 2J).

3.3. The HF and/or HC diets worsened Stx2-induced neurodegeneration

NeuN was used as a biomarker to determine neurodegenerative events [24] in VA-VL thalamus (Fig. 3A). Conserved NeuN immunofluorescence was detected in veh-treated neuronal nuclei (Fig. 3B, arrowhead). A non-significant number of abnormal thalamic nuclei was detected in veh-treated groups regardless of diets (Table 5, Fig. 3K), all of them showing conserved NeuN immunofluorescence colocalizing with Hoechst staining (Fig. 3B–D, F, H, K, see arrowhead in B). In contrast, Stx2-treated groups showed significant aberrant neurodegenerative neuronal phenotypes (Fig. 3C–E, G, I). A neurodegenerative profile is characterized by

Table 2
Number of microvessels bound to lectins; $p = 0.0001$.

ND + veh	ND + Stx2	HF + veh	HF + Stx2
28.82 ± 4.45	43.29 ± 5.24	31.41 ± 3.11	52.06 ± 6.24
HC + veh	HC + Stx2	HF + HC + veh	HF + HC + Stx2
30.29 ± 4.57	57.94 ± 9.89	31.53 ± 4.12	72.65 ± 11

Table 3
Microvessel size (um^2); p = 0.0001.

ND + veh	ND + Stx2	HF + veh	HF + Stx2
165.86 ± 30.32	107.63 ± 31.58	145.27 ± 17.30	81.27 ± 18.71
HC + veh	HC + Stx2	HF + HC + veh	HF + HC + Stx2
142.63 ± 18.87	57.27 ± 11.99	139.27 ± 19.14	46.57 ± 8.23

Table 4
total area occupied by microvessels (%); p = 0.0001.

ND + veh	ND + Stx2	HF + veh	HF + Stx2
18.41 ± 2.53	10.31 ± 1.95	17.05 ± 2.88	8.52 ± 0.78
HC + veh	HC + Stx2	HF + HC + veh	HF + HC + Stx2
17.36 ± 2.90	5.71 ± 1.00	16.77 ± 2.27	3.13 ± 1.13

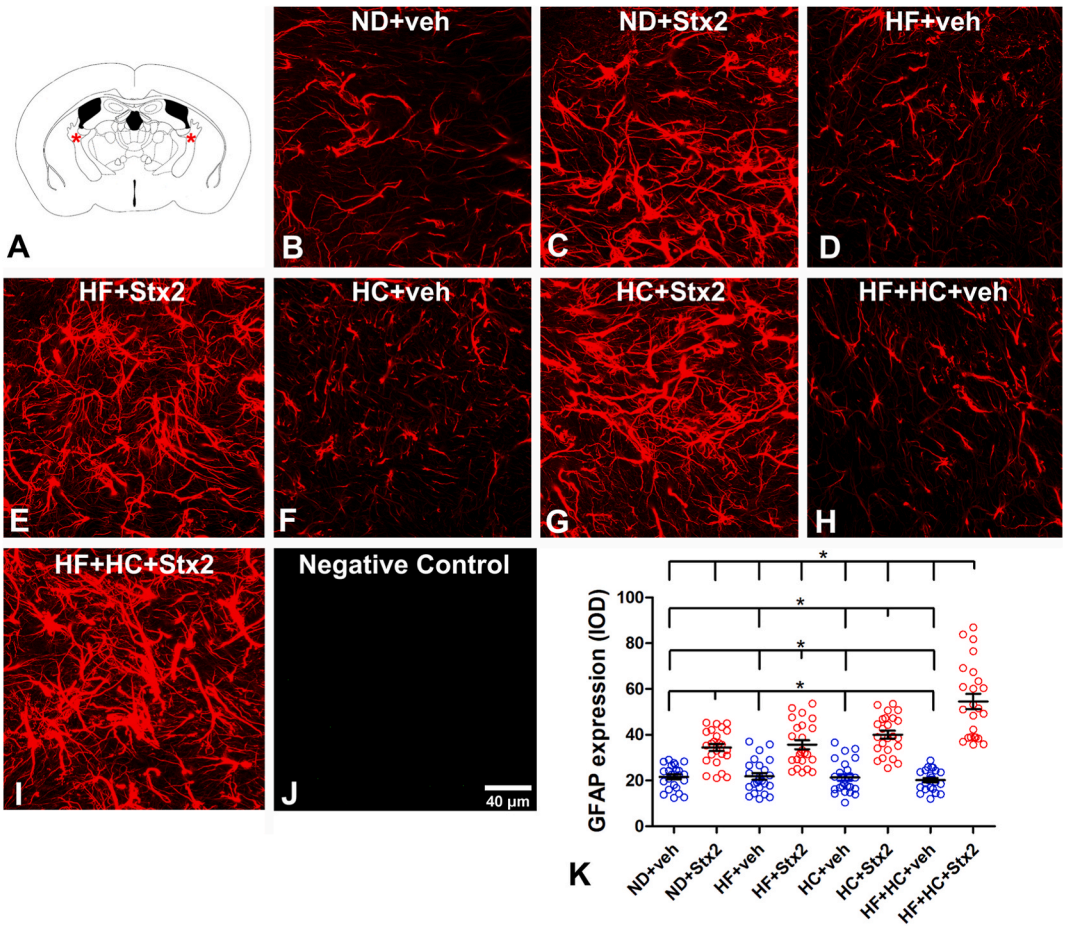

Fig. 2. Changes in astrocyte GFAP expression. A: the murine internal capsule brain area studied; B: micrograph shows the astrocyte expression of GFAP in the ND + veh control group; C: ND + Stx2 treatment; D: HF + veh treatment; E: HF + Stx2 treatment; F: HC + veh treatment; G: HC + Stx2 treatment; H: HF + HC + veh treatment; I: HF + HC + Stx2 treatment; J: negative control by omitting primary antibody; K: quantification of GFAP expression levels in all treatments. Data were analyzed by one-way ANOVA and Bonferroni post hoc test, p = 0.0001, n = 5. Scale bar in J applies to all panels.

Table 5
Astrocyte reactivity (IOD); p = 0.0001.

ND + veh	ND + Stx2	HF + veh	HF + Stx2
21.65 ± 5.20	34.50 ± 7.68	21.83 ± 7.20	35.68 ± 9.66
HC + veh	HC + Stx2	HF + HC + veh	HF + HC + Stx2
21.38 ± 7.07	40.08 ± 8.49	20.23 ± 4.48	54.53 ± 16.42

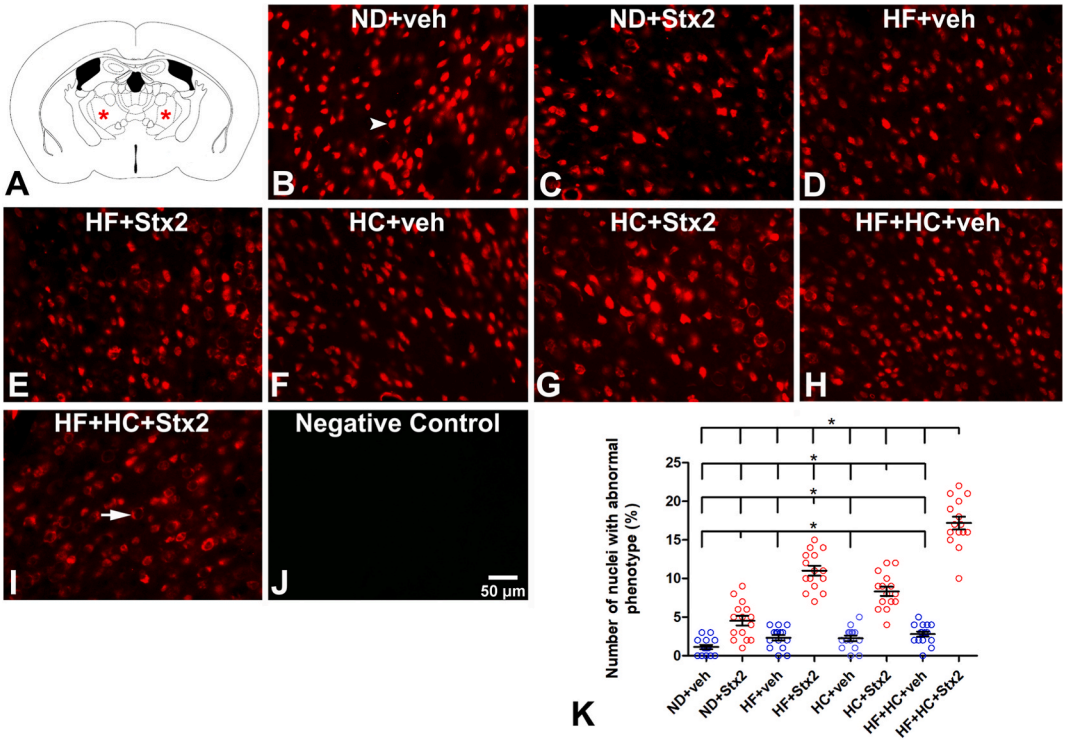

Fig. 3. Changes in the neuron NeuN fluorescence patterns. A: the murine VA-VL brain area studied; B: micrograph shows NeuN localization in the ND + veh control group; C: ND + Stx2 treatment; D: HF + veh treatment; E: HF + Stx2 treatment; F: HC + veh treatment; G: HC + Stx2 treatment; H: HF + HC + veh treatment; I: HF + HC + Stx2 treatment; J: negative control by omitting primary antibody; K: quantification of nuclei with abnormal phenotypes in all treatments. Arrowhead in B: normal phenotype; arrow in I: abnormal phenotype. Data were analyzed by one-way ANOVA and Bonferroni post hoc test, p = 0.0001, n = 5. Scale bar in J applies to all panels.

positive NeuN immunofluorescence in the perinuclear area and negative in the nucleus (Fig. 3I, arrow). Most neurons in degenerative state were found in the HF + HC + Stx2 group (Table 6, Fig. 3K). Negative controls lacked NeuN immunofluorescence (Fig. 3J).

3.4. The HF + HC diet boosted Stx2-induced microglia reactivity

As Iba1 is a microglia/macrophage-specific calcium-binding protein and a marker of activated microglia [25], Iba1 expression levels were used to assess microglial activation in the VA-VL thalamus (Fig. 4A). A significant rise was observed in Iba1 expression in HC + veh and HF + HC + veh in comparison with ND + veh (Table 7, Fig. 4B–D, F, H, K). At variance, a significant increase in Iba1 expression levels was found in all four Stx2 groups (Table 7, Fig. 4C–E, G, I, K). The maximal increase in Iba1 expression was observed in the HC + HF + Stx2 condition (Fig. 4I–K). A negative control for IBA1 immunofluorescence obtained by suppressing the primary

Table 6
Number of nuclei with abnormal phenotype; p = 0.0001.

ND + veh	ND + Stx2	HF + veh	HF + Stx2
1.13 ± 1.06	4.53 ± 2.39	2.33 ± 1.35	11.00 ± 2.45
HC + veh	HC + Stx2	HF + HC + veh	HF + HC + Stx2
2.27 ± 1.39	8.33 ± 2.29	2.80 ± 1.32	17.20 ± 3.12

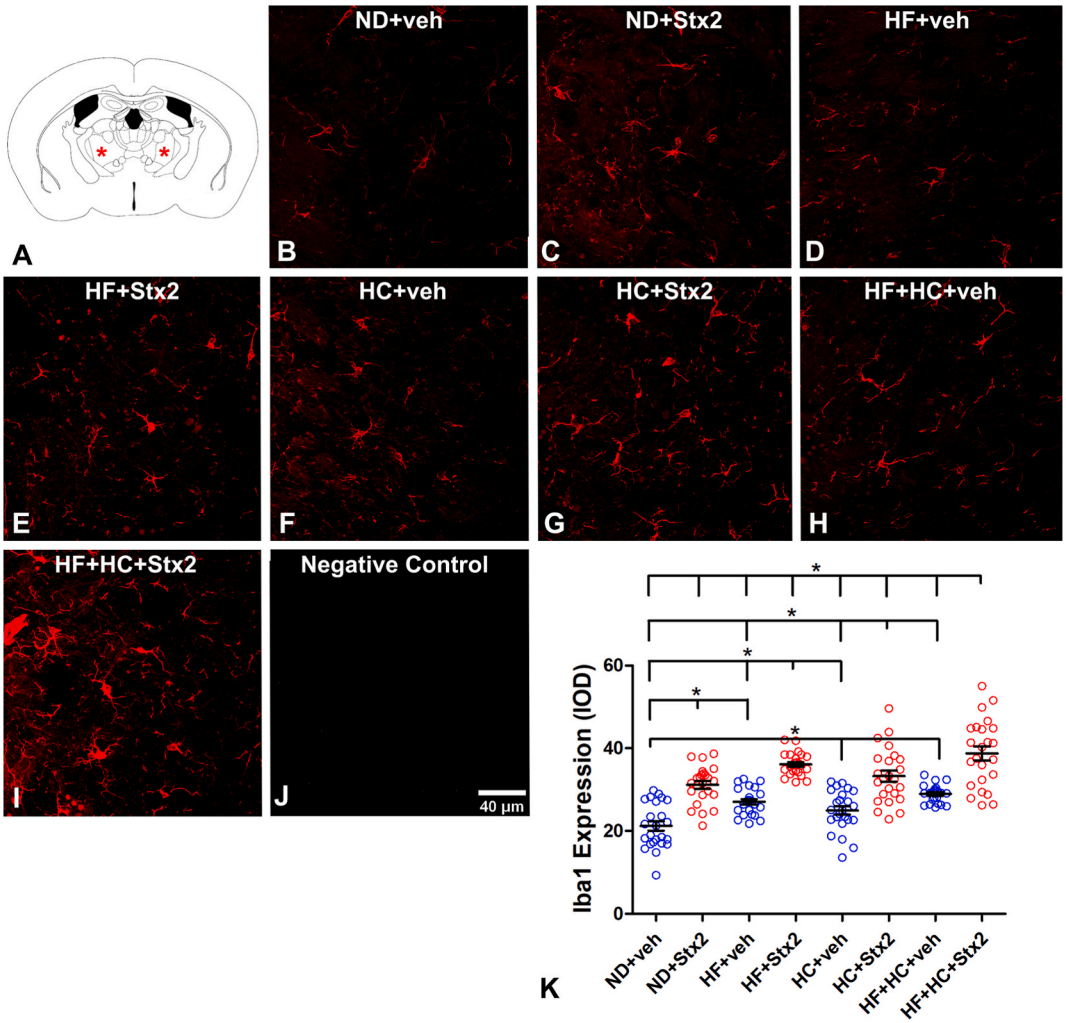

Fig. 4. Changes in Iba1 expression and number of Iba1-positive cells. A: the murine VA-VL brain area studied; B: micrograph shows the expression of Iba1 and the number of Iba1-positive cells in the ND + veh control group; C: ND + Stx2 treatment; D: HF + veh treatment; E: HF + Stx2 treatment; F: HC + veh treatment; G: HC + Stx2 treatment; H: HF + HC + veh treatment; I: HF + HC + Stx2 treatment; J: negative control by omitting primary antibody; K: quantification of Iba1 expression levels in all treatments. Data were analyzed by one-way ANOVA and Bonferroni post hoc test, $p = 0.0001$, $n = 5$. Scale bar in J applies to all panels.

Table 7
microglial reactivity (IOD); $p = 0.0001$.

ND + veh	ND + Stx2	HF + veh	HF + Stx2
21.21 ± 5.47	31.17 ± 4.53	27.05 ± 3.20	36.14 ± 2.74
HC + veh	HC + Stx2	HF + HC + veh	HF + HC + Stx2
24.91 ± 4.96	33.26 ± 6.67	28.95 ± 2.13	38.75 ± 8.18

antibody revealed negative immunofluorescence (Fig. 4J).

3.5. The HF + HC diet deepened Stx2-induced reduction in oligodendrocyte MBP expression

MBP is a myelin sheath protein whose loss is considered a marker of myelin degeneration [26]. For this reason, changes in MBP expression were assessed in the internal capsule (Fig. 5A) to determine myelin degeneration following diets and treatments. We have previously shown that Stx2 reduces the expression of MBP in mice following a regular diet [27,28]. In this study, no significant differences were observed across veh-treated groups (Table 8, Fig. 5K). However, all Stx2 groups underwent a significant reduction in

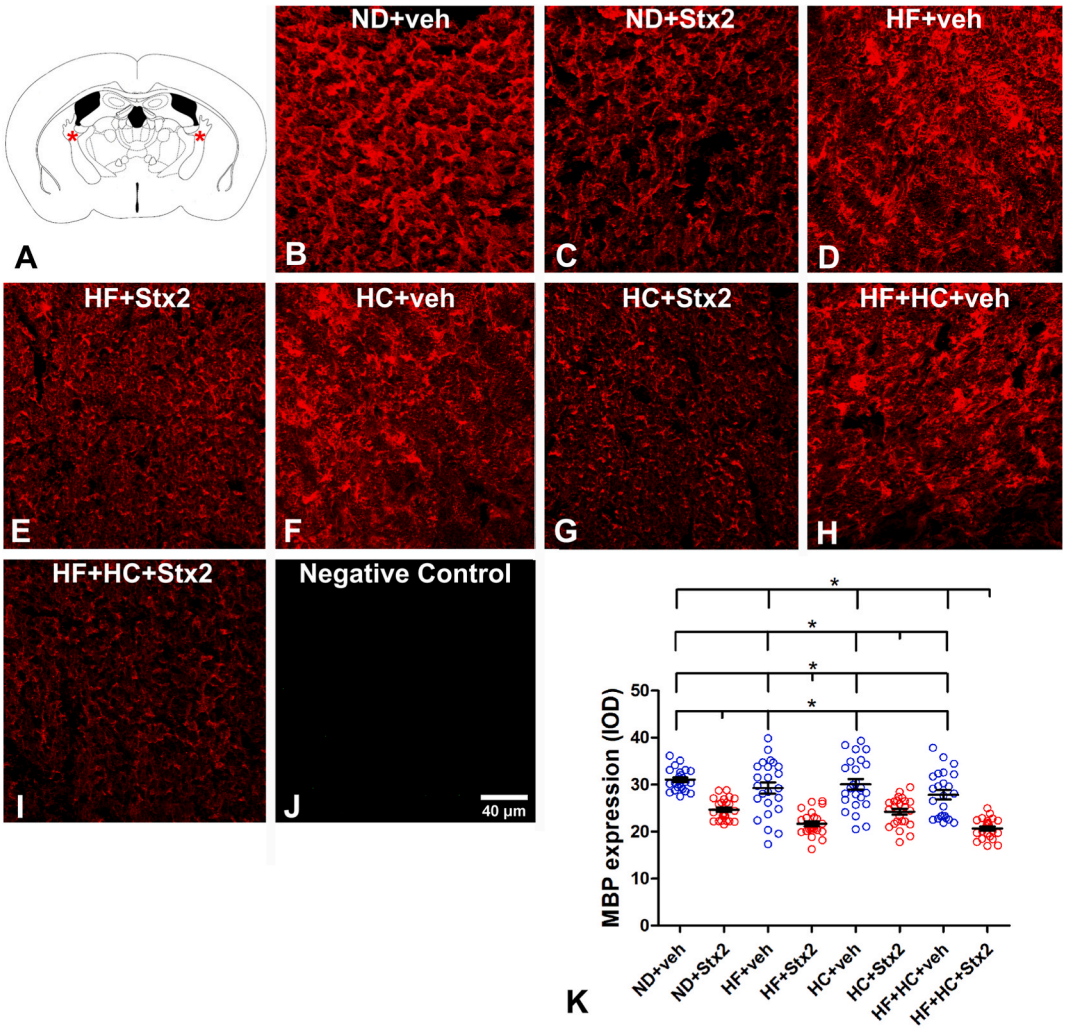

Fig. 5. Changes in MBP expression. A: the murine internal capsule brain area studied; B: micrograph shows the expression of MBP in the ND + veh control group; C: ND + Stx2 treatment; D: HF + veh treatment; E: HF + Stx2 treatment; F: HC + veh treatment; G: HC + Stx2 treatment; H: HF + HC + veh treatment; I: HF + HC + Stx2 treatment; J: negative control by omitting primary antibody; K: quantification of MBP expression levels in all treatments. Data were analyzed by one-way ANOVA and Bonferroni post hoc test, $p < 0.005$, $n = 5$. Scale bar in J applies to all panels.

Table 8
MBP expression (IOD); $p = 0.0001$.

ND + veh	ND + Stx2	HF + veh	HF + Stx2
31.05 ± 2.27	24.65 ± 2.28	29.30 ± 5.87	21.68 ± 2.56
HC + veh	HC + Stx2	HF + HC + veh	HF + HC + Stx2
30.10 ± 5.44	24.23 ± 3.08	27.85 ± 4.88	20.69 ± 2.09

MBP expression (Fig. 5K), with the minimum value observed in HF + HC + Stx2 animals (Table 8). No MBP immunofluorescence was observed in negative controls (Fig. 5J).

3.6. The HF + HC diet lowered the motor performance in the context of Stx2

A swim motor evaluation was carried out in mice (Fig. 6A) to establish whether cellular damage induced by Stx2 and deepened by the HF and/or HC diets correlated with neurological motor alterations [29]. All Stx2-treated groups required significantly more time to reach the platform than their respective veh-treated groups (Fig. 6B). No significant differences in latency were found across Stx2-treated groups, although a non-significant peak was observed in the HF + HC + Stx2 group, indicative of motor deficits (Table 9,

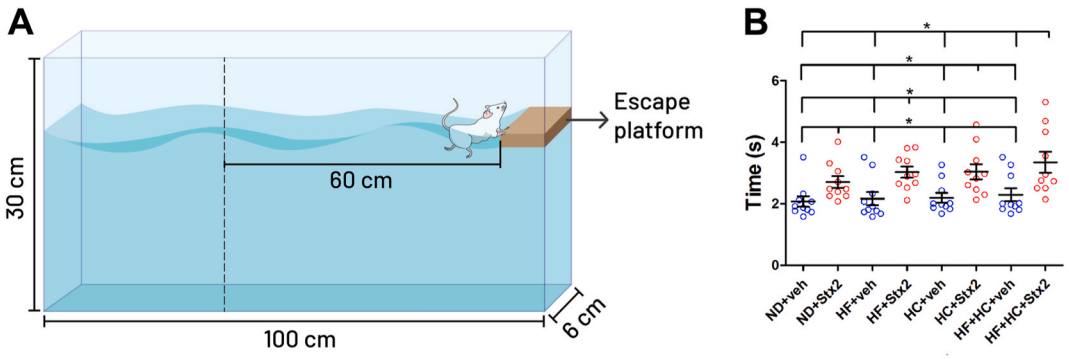

Fig. 6. Changes in mouse motor behavior. A: design of the test device; B: columns indicate the different treatments. Data were analyzed by one-way ANOVA and Bonferroni post hoc test, p = 0.0001, n = 10.

Table 9
latency time (seconds); p = 0.0001.

ND + veh	ND + Stx2	HF + veh	HF + Stx2
2.07 ± 0.55	2.70 ± 0.60	2.17 ± 0.68	3.03 ± 0.57
HC + veh	HC + Stx2	HF + HC + veh	HF + HC + Stx2
2.19 ± 0.52	3.04 ± 0.79	2.29 ± 0.67	3.35 ± 1.08

Fig. 6B).

3.7. Stx2 affected mouse sensitivity without diet involvement

As neurological motor performance was hindered in mice treated with Stx2, we next evaluated mouse sensitivity using Von Frey filaments (Fig. 7A). Changes in paw withdrawal to mechanical stimuli with different filament sizes determine the degree of alterations in sensitivity [30]. No significant differences were found in mouse paw sensitivity across Stx2-treated groups (Fig. 7B). Worth pointing out, stronger filaments were used in Stx2-treated animals, which reflects significantly lower sensitivity in Stx2 groups as compared to their respective veh-treated groups (Table 10, Fig. 7B).

4. Discussion

The present findings demonstrate the implications of a poor diet, which may define the health condition of patients intoxicated with STEC. To the best of our knowledge, the results presented here are novel, as they demonstrate the relevance of nutrition in encephalopathy triggered by Stx2 for the first time. These data could explain why, given a STEC outbreak, some patients suffer extreme, potentially lethal neurological alterations, while others present only mild and reversible symptoms [10]. Previous reports have demonstrated that high-fat and high-sugar diets promote cognitive and behavioral alterations, together with an increase in systemic and local proinflammatory cytokines [31,32]. In the present study, the HC and HF diets worsened the damage produced by Stx2 in the mouse motor thalamus and internal capsule. These findings were obtained at a cellular level, with microvessel profile alterations and astrocyte and microglial reactivity. Neurodegeneration and myelin protein alterations were concomitantly observed, all indicative of a pathological state. Similar findings on peripheral sensory-motor dysfunctions and neurodegeneration in the context of reactive pro-inflammatory microglia have been reported in brain areas in a model of aging mice subjected to a western diet – high-fat, high-sugar, and high-salt– [33]. Similarly, elderly rats subjected to a high-fat, high-sugar diet evidenced impaired spatial learning and working memory and increased anxiety-like behavior, associated with decreased neurogenesis and increased neuroinflammation fostered by astrogliosis [34]. Furthermore, a model of metabolic syndrome has revealed a proinflammatory state – including exacerbated oxidative stress and neuronal damage– in reptilian and limbic murine brain regions, resulting in recognition memory loss [35].

Microbiota, the intestine, and the brain interact in a multidirectional way, mainly through the vagus nerve. The afferent fibers of the vagus nerve constitute the main parasympathetic link of the gut-brain axis, as their axonal terminals in the intestinal mucosa sense the mediators released by intestinal epithelial cells, as well as substances released by intestinal bacteria such as LPS [36–38]. It has been established that dietary habits influence intestinal microbiome diversity and can induce profound changes in brain homeostasis. These changes may be mediated by microglial activation, systemic inflammation, and vagal afferent signaling, culminating in neuroinflammation. Eating habits have changed significantly in recent years toward a diet rich in processed fats and low in fibers and other functional components of foods. This diet, commonly referred to as western diet, favors the development of metabolic alterations in multiple organs including the CNS [39]. The intestine is first damaged, as a western diet alters its ability to function as a barrier against

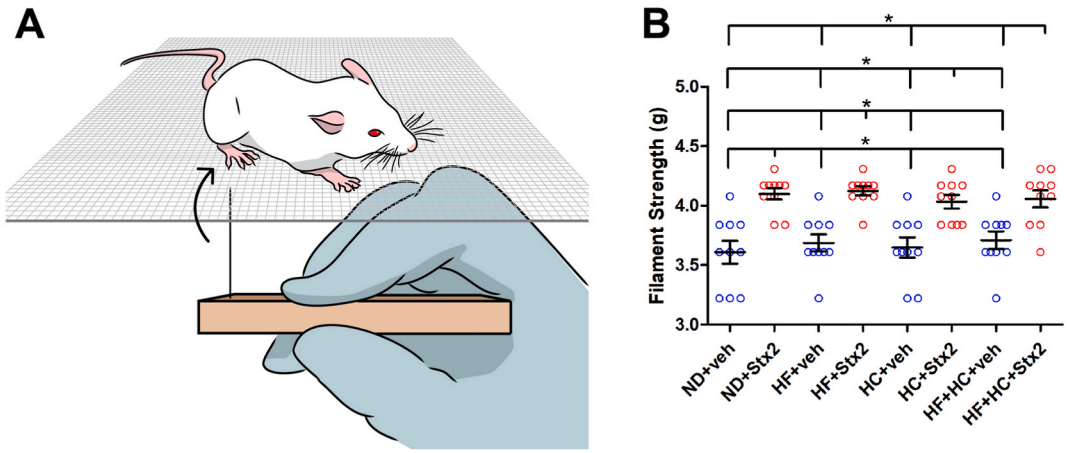

Fig. 7. Changes in mouse sensitivity. A: design of the test device; B: columns indicate the different treatments. Data were analyzed by one-way ANOVA and Bonferroni post hoc test, p = 0.0001, n = 10.

Table 10
sensitivity (grams); p = 0.0001.

ND + veh	ND + Stx2	HF + veh	HF + Stx2
3.61 ± 0.30	4.1 ± 0.15	3.69 ± 0.23	4.12 ± 0.12
HC + veh	HC + Stx2	HF + HC + veh	HF + HC + Stx2
3.65 ± 0.27	4.03 ± 0.18	3.71 ± 0.23	4.06 ± 0.23

pathogenic microorganisms and toxins [40]. Indeed, recent work has linked this type of diet with dysbiosis characterized by the proliferation of enterobacteria, including strains of adherent-invasive E. coli (AIEC) [41]. This larger proportion of gut-resident Enterobacteriaceae may trigger susceptibility to infection by phages carrying the Stx gene [42], as these lysogenic strain derivatives can be a source of Stx. In addition, Enterobacteriaceae act as a source of LPS, favoring the development of a chronic, subclinical pro-inflammatory state which increases Stx-associated toxicity [43]. Furthermore, high-fat, high-carbohydrate diets can stimulate the deleterious TLR4 inflammatory pathway by increasing LPS translocation and modulating brain functions [44,45].

In addition to an adequate balance of macronutrients, especially fats and sugars, abundant research suggests that bioactive components present in food contribute to the proliferation of bacteria and promote the distribution of microbial communities, which can maintain homeostasis in the intestinal microenvironment and the brain-gut-microbiota axis [46].

Considering the results presented, it may be concluded that malnourished children intoxicated with STEC-HUS are more susceptible to severe encephalopathy produced by Stx2. Indeed, malnourished children are more likely to suffer inflammation in the gut, the weakening of the mucosa barrier, an immune reaction, and dysbiosis, all of which generate more toxic bacterial products that enter circulation, alter the blood brain barrier, and ultimately damage brain function and structure. These conclusions are in line with previous reports based on malnourished children [47] and adolescent studies [48]. It should be noted that other types of malnutrition may alter child behavior in different ways, as an unbalanced diet fails to provide the nutrients required, both qualitatively and quantitatively. For example, lower intake of folate and B vitamins has been shown to correlate with violent and delinquent behavior in adolescents [48]. Altogether, this evidence raises an extensive and complex issue which requires significant efforts in research and policy making to eradicate malnutrition.

5. Conclusions

Thalamic and internal capsule cellular alterations correlated with neurological motor dysfunction and loss of sensitivity following unbalanced high-fats and high-carbohydrate diets. This work thus demonstrates that malnutrition should be considered a risk factor which may define disease severity following Stx2 intoxication.

CRediT authorship contribution statement

D. Arenas-Mosquera: Visualization, Methodology, Investigation, Formal analysis. **N. Cerny:** Methodology, Investigation, Formal analysis. **A. Cangelosi:** Methodology, Investigation. **P.A. Geoghegan:** Formal analysis. **E.L. Malchiodi:** Formal analysis. **M. De Marzi:** Writing – original draft, Formal analysis. **A. Pinto:** Visualization, Methodology, Investigation, Formal analysis, Data curation. **J. Goldstein:** Writing – original draft, Funding acquisition, Conceptualization.

Ethics approval

Experimental protocols and euthanasia procedures were reviewed and approved by the Institutional Animal Care and Use Committee of the School of Medicine at Universidad de Buenos Aires, Argentina (Resolution N° 3020/2019). All the procedures were performed in accordance with the ARRIVE and EEOC guidelines for the care and use of experimental animals (EEC Council 86/609).

Consent for publication

N/A.

Availability of data and materials

Data associated with this study are available in the supplemental materials and a public repository at: bioRxiv 2024.02.06.579171; doi: https://doi.org/10.1101/2024.02.06.579171.

Funding

This work was supported by Agencia Nacional de Promoción Científica y Tecnológica (ANPCyT) (PICT-2021-00656), Universidad de Buenos Aires (UBACyT) (20020190100186BA), and Consejo Nacional de Investigaciones Científicas y Técnicas (CONICET) (PIP 11220200101293CO), Argentina.

Declaration of competing interest

There are no potential competing interests, all coauthors have read and agreed to the content of the manuscript. The content of the manuscript has not been publishedor submitted for publication elsewhere.

Acknowledgments

We wish to thank German La Iacona for his invaluable technical advice and support in capturing fluorescent micrographs of this work.

List of abbreviations

ANOVA one-way analysis of variance
anti-GFAP glial fibrillary acidic protein antibody
anti-Iba1 ionized calcium binding adaptor molecule 1 antibody
anti-NeuN neuronal nuclei antibody
Gb3 globotriaosylceramide
HC diet high in carbohydrates
HC + Stx2 diet high in carbohydrates treated with i.v Shiga toxin 2
HC + veh diet high in carbohydrates treated with i.v vehicle
HC + HF diet high in carbohydrates and high in fats
i.v intravenous
HF diet high in fats
HF + Stx2 diet high in fats treated with iv. Shiga toxin 2
HF + veh diet high in fats treated with iv. vehicle
HC + HF + Stx2 diet high in carbohydrates and high in fats treated with i.v Shiga toxin 2
HC + HF + veh diet high in carbohydrates and high in fats treated with i.v vehicle
HUS hemolytic uremic syndrome
IOD integrated optical density
anti-MBP myelin basic protein antibody
ND normal diet
ND + Stx2 normal diet treated with i.v Shiga toxin 2
ND + veh normal diet treated with i.v vehicle
PBS phosphate saline buffer
STEC Stx producing *E. coli*
Stx2 Shiga toxin 2
VA-VL ventral anterior and ventral lateral nuclei
veh vehicle

Appendix A. Supplementary data

Supplementary data to this article can be found online at https://doi.org/10.1016/j.heliyon.2024.e39871.

References

[1] A. Pinto, A.B. Celi, J. Goldstein, Shiga toxin and its effect on the central nervous system, in: A.G. Torres (Ed.), Trending Topics in Escherichia coli Research: the Latin American Perspective, Springer International Publishing, Cham, 2023, pp. 177–204.
[2] M.E. Del Cogliano, A. Pinto, J. Goldstein, E. Zotta, F. Ochoa, R.J. Fernandez-Brando, et al., Relevance of bacteriophage 933W in the development of hemolytic uremic syndrome (HUS), Front. Microbiol. 9 (2018) 3104.
[3] L.V. Bentancor, M.P. Mejias, A. Pinto, M.F. Bilen, R. Meiss, M.C. Rodriguez-Galan, et al., Promoter sequence of Shiga toxin 2 (Stx2) is recognized in vivo, leading to production of biologically active Stx2, mBio 4 (5) (2013) e00501–e00513.
[4] G. Cabrera, R.J. Fernandez-Brando, M.J. Abrey-Recalde, A. Baschkier, A. Pinto, J. Goldstein, et al., Retinoid levels influence enterohemorrhagic Escherichia coli infection and Shiga toxin 2 susceptibility in mice, Infect. Immun. 82 (9) (2014) 3948–3957.
[5] A.B. Celi, J. Goldstein, M.V. Rosato-Siri, A. Pinto, Role of globotriaosylceramide in Physiology and pathology, Front. Mol. Biosci. 9 (2022) 813637.
[6] F. Obata, K. Tohyama, A.D. Bonev, G.L. Kolling, T.R. Keepers, L.K. Gross, et al., Shiga toxin 2 affects the central nervous system through receptor globotriaosylceramide localized to neurons, J. Infect. Dis. 198 (9) (2008) 1398–1406.
[7] M. Shimizu, Pathogenic functions and diagnostic utility of cytokines/chemokines in EHEC-HUS, Pediatr. Int. 62 (3) (2020) 308–315.
[8] D. Arenas-Mosquera, A. Pinto, N. Cerny, C. Berdasco, A. Cangelosi, P.A. Geoghegan, et al., Cytokines expression from altered motor thalamus and behavior deficits following sublethal administration of Shiga toxin 2a involve the induction of the globotriaosylceramide receptor, Toxicon 216 (2022) 115–124.
[9] A. Pinto, A. Cangelosi, P.A. Geoghegan, J. Goldstein, Dexamethasone prevents motor deficits and neurovascular damage produced by shiga toxin 2 and lipopolysaccharide in the mouse striatum, Neuroscience 344 (2017) 25–38.
[10] A.G. Torres, M.M. Amaral, L. Bentancor, L. Galli, J. Goldstein, A. Kruger, et al., Recent advances in shiga toxin-producing Escherichia coli research in Latin America, Microorganisms 6 (4) (2018).
[11] J. Goldstein, K. Nunez-Goluboay, A. Pinto, Therapeutic strategies to protect the central nervous system against shiga toxin from enterohemorrhagic Escherichia coli, Curr. Neuropharmacol. 19 (1) (2021) 24–44.
[12] F. Obata, Influence of Escherichia coli Shiga toxin on the mammalian central nervous system, Adv. Appl. Microbiol. 71 (2010) 1–19.
[13] C. Tironi-Farinati, P.A. Geoghegan, A. Cangelosi, A. Pinto, C.F. Loidl, J. Goldstein, A translational murine model of sub-lethal intoxication with Shiga toxin 2 reveals novel ultrastructural findings in the brain striatum, PLoS One 8 (1) (2013) e55812.
[14] T. Magnus, J. Rother, O. Simova, M. Meier-Cillien, J. Repenthin, F. Moller, et al., The neurological syndrome in adults during the 2011 northern German E. coli serotype O104:H4 outbreak, Brain 135 (Pt 6) (2012) 1850–1859.
[15] J. Kramer, M. Deppe, K. Gobel, K. Tabelow, H. Wiendl, S.G. Meuth, Recovery of thalamic microstructural damage after Shiga toxin 2-associated hemolytic-uremic syndrome, J. Neurol. Sci. 356 (1–2) (2015) 175–183.
[16] S.G. Meuth, K. Gobel, T. Kanyshkova, P. Ehling, M.A. Ritter, W. Schwindt, et al., Thalamic involvement in patients with neurologic impairment due to Shiga toxin 2, Ann. Neurol. 73 (3) (2013) 419–429.
[17] B. Bojkova, P.J. Winklewski, M. Wszedybyl-Winklewska, Dietary fat and cancer-which is good, which is bad, and the body of evidence, Int. J. Mol. Sci. 21 (11) (2020).
[18] G. Paxinos, K.B.J. Franklin, The Mouse Brain in Stereotaxic Coordinates, Academic Press, 2001.
[19] M. Catani, M. Thiebaut de Schotten, A diffusion tensor imaging tractography atlas for virtual in vivo dissections, Cortex 44 (8) (2008) 1105–1132.
[20] R.J. Carter, L.A. Lione, T. Humby, L. Mangiarini, A. Mahal, G.P. Bates, S.B. Dunnett, A.J. Morton, Characterization of progressive motor deficits in mice transgenic for the human Huntington's disease mutation, J. Neurosci. 19 (8) (1999 Apr 15) 3248–3257.
[21] G.A. Lambert, G. Mallos, A.S. Zagami, Von Frey's hairs–a review of their technology and use–a novel automated von Frey device for improved testing for hyperalgesia, J. Neurosci. Methods 177 (2) (2009 Mar 15) 420–426.
[22] R. Piña, A.I. Santos-Díaz, E. Orta-Salazar, A.R. Aguilar-Vazquez, C.A. Mantellero, I. Acosta-Galeana, A. Estrada-Mondragon, M. Prior-Gonzalez, J.I. Martinez-Cruz, A. Rosas-Arellano, Ten approaches that improve immunostaining: a review of the latest advances for the optimization of immunofluorescence, Int. J. Mol. Sci. 23 (3) (2022 Jan 26) 1426.
[23] A.W. Toga, Brain Mapping: an Encyclopedic Reference, Elsevier/Academic Press, 2015.
[24] C.L. Robertson, A. Puskar, G.E. Hoffman, A.Z. Murphy, M. Saraswati, G. Fiskum, Physiologic progesterone reduces mitochondrial dysfunction and hippocampal cell loss after traumatic brain injury in female rats, Exp. Neurol. 197 (1) (2006) 235–243.
[25] C. Berdasco, A. Pinto, M.G. Blake, F. Correa, N.A.L. Carbajosa, A.B. Celi, et al., Cognitive deficits found in a pro-inflammatory state are independent of ERK1/2 signaling in the murine brain Hippocampus treated with shiga toxin 2 from enterohemorrhagic Escherichia coli, Cell. Mol. Neurobiol. 43 (5) (2023) 2203–2217.
[26] M.T. Weil, W. Mobius, A. Winkler, T. Ruhwedel, C. Wrzos, E. Romanelli, et al., Loss of myelin basic protein function triggers myelin breakdown in models of demyelinating diseases, Cell Rep. 16 (2) (2016) 314–322.
[27] C. Berdasco, A. Pinto, V. Calabro, D. Arenas, A. Cangelosi, P. Geoghegan, et al., Shiga toxin 2 from enterohemorrhagic Escherichia coli induces reactive glial cells and neurovascular disarrangements including edema and lipid peroxidation in the murine brain hippocampus, J. Biomed. Sci. 26 (1) (2019) 16.
[28] A. Pinto, C. Berdasco, D. Arenas-Mosquera, A. Cangelosi, P.A. Geoghegan, M.C. Nunez, et al., Anti-inflammatory agents reduce microglial response, demyelinating process and neuronal toxin uptake in a model of encephalopathy produced by Shiga Toxin 2, Int J Med Microbiol 308 (8) (2018) 1036–1042.
[2][9] S.M. Sherman, The thalamus is more than just a relay, Curr. Opin. Neurobiol. 17 (4) (2007) 417–422.
[30] H. Teng, S. Chen, K. Fan, Q. Wang, B. Xu, D. Chen, F. Zhao, T. Wang, Dexamethasone liposomes alleviate osteoarthritis in miR-204/-211-deficient mice by repolarizing synovial macrophages to M2 phenotypes, Mol. Pharm. 20 (8) (2023 Aug 7) 3843–3853.
[31] J.E. Beilharz, J. Maniam, M.J. Morris, Short exposure to a diet rich in both fat and sugar or sugar alone impairs place, but not object recognition memory in rats, Brain Behav. Immun. 37 (2014) 134–141.
[32] G. Jamar, D.A. Ribeiro, L.P. Pisani, High-fat or high-sugar diets as trigger inflammation in the microbiota-gut-brain axis, Crit. Rev. Food Sci. Nutr. 61 (5) (2021) 836–854.
[33] S. Hong, A. Nagayach, Y. Lu, H. Peng, Q.A. Duong, N.B. Pham, et al., A high fat, sugar, and salt Western diet induces motor-muscular and sensory dysfunctions and neurodegeneration in mice during aging: ameliorative action of metformin, CNS Neurosci. Ther. 27 (12) (2021) 1458–1471.
[34] B. Mota, M. Ramos, S.I. Marques, A. Silva, P.A. Pereira, M.D. Madeira, et al., Effects of high-fat and high-fat high-sugar diets in the anxiety, learning and memory, and in the Hippocampus neurogenesis and neuroinflammation of aged rats, Nutrients 15 (6) (2023).
[35] E. Fuentes, B. Venegas, G. Munoz-Arenas, C. Moran, R.A. Vazquez-Roque, G. Flores, et al., High-carbohydrate and fat diet consumption causes metabolic deterioration, neuronal damage, and loss of recognition memory in rats, J. Chem. Neuroanat. 129 (2023) 102237.
[36] C.B. de La Serre, G. de Lartigue, H.E. Raybould, Chronic exposure to low dose bacterial lipopolysaccharide inhibits leptin signaling in vagal afferent neurons, Physiol. Behav. 139 (2015) 188–194.
[37] P. Forsythe, W. Kunze, J. Bienenstock, Moody microbes or fecal phrenology: what do we know about the microbiota-gut-brain axis? BMC Med. 14 (2016) 58.
[38] B. Bonaz, Is-there a place for vagus nerve stimulation in inflammatory bowel diseases? Bioelectron Med 4 (2018) 4.

[39] C. Contreras, I. Gonzalez-Garcia, N. Martinez-Sanchez, P. Seoane-Collazo, J. Jacas, D.A. Morgan, et al., Central ceramide-induced hypothalamic lipotoxicity and ER stress regulate energy balance, Cell Rep. 9 (1) (2014) 366–377.
[40] S.C. Bischoff, G. Barbara, W. Buurman, T. Ockhuizen, J.D. Schulzke, M. Serino, et al., Intestinal permeability–a new target for disease prevention and therapy, BMC Gastroenterol. 14 (2014) 189.
[41] A. Agus, J. Denizot, J. Thevenot, M. Martinez-Medina, S. Massier, P. Sauvanet, et al., Western diet induces a shift in microbiota composition enhancing susceptibility to Adherent-Invasive E. coli infection and intestinal inflammation, Sci. Rep. 6 (2016) 19032.
[42] N.A. Cornick, A.F. Helgerson, V. Mai, J.M. Ritchie, D.W. Acheson, In vivo transduction of an Stx-encoding phage in ruminants, Appl. Environ. Microbiol. 72 (7) (2006) 5086–5088.
[43] L.M. Harrison, D.W. Gaines, U.S. Babu, K.V. Balan, R. Reimschuessel, A.B. Do, et al., Diet-induced obesity precipitates kidney dysfunction and alters inflammatory mediators in mice treated with Shiga Toxin 2, Microb. Pathog. 123 (2018) 250–258.
[44] P. Forsythe, W.A. Kunze, Voices from within: gut microbes and the CNS, Cell. Mol. Life Sci. 70 (1) (2013) 55–69.
[45] P. Brun, M.C. Giron, M. Qesari, A. Porzionato, V. Caputi, C. Zoppellaro, et al., Toll-like receptor 2 regulates intestinal inflammation by controlling integrity of the enteric nervous system, Gastroenterology 145 (6) (2013) 1323–1333.
[46] T.G. Dinan, J.F. Cryan, Gut instincts: microbiota as a key regulator of brain development, ageing and neurodegeneration, J Physiol. 595 (2) (2017) 489–503.
[47] R.B. Oriá, L.E. Murray-Kolb, R.J. Scharf, L.L. Pendergast, D.R. Lang, G.L. Kolling, R.L. Guerrant, Early-life enteric infections: relation between chronic systemic inflammation and poor cognition in children, Nutr. Rev. 74 (6) (2016 Jun) 374–386.
[48] J.R. Galler, J.R. Koethe, R.H. Yolken, Neurodevelopment: the impact of nutrition and inflammation during adolescence in low-resource settings, Pediatrics 139 (Suppl 1) (2017 Apr) S72–S84, https://doi.org/10.1542/peds.2016-2828I. PMID: 28562250; PMCID: PMC5374755.